ISSN:2319-9873

Research & Reviews: Journal of Engineering and Technology

Numerical Study of Convective Heat Transfer for Different Shapes of Hot Sources Inside an Enclosure

Balamurugan S[1]* and Krishnakanth K[2]

[1]Assistant Professor, Department of Mechanical Engineering, Coimbatore Institute of Technology, Coimbatore – 641 014, Tamilnadu, India.

[2]Post Graduate Student, Heat Power Engineering, Coimbatore Institute of Technology, Coimbatore – 641 014, Tamilnadu, India.

Research Article

Received date: 27/07/2015

Accepted date: 13/09/2015

Published date: 25/09/2015

***For Correspondence**

Balamurugan S, Assistant Professor, Department of Mechanical Engineering, Coimbatore Institute of Technology, Coimbatore – 641 014, Tamilnadu, India. Tel: +91-(0)-9865062725.

E-mail: balu74_cit@yahoo.co.in

Keywords

Natural convection, Numerical simulation, Comparison.

ABSTRACT

In this paper, natural convection around a square and triangle bar kept in a square enclosure has been studied. Aim of this research has analysis, the heat transfer based on natural convection by using air as a medium. The problems taken for study were a varying square enclosure with different aspect ratio of sources of both square and triangle bar. Numerical simulations and boundary conditions are carried out for analysis these systems by using Fluent Software. The square and triangle bar are considered as a hot source and the square enclosure of vertical walls are cold surfaces and horizontal walls are insulated. The size of the square enclosure are taken 20 mm, 40 mm and 80 mm corresponding to each enclosure were taken as the aspect ratio of both square and triangle bar of 0.2, 0.3 and 0.4 respectively. The heat transfer results are obtained from simulation with the help of temperature distribution, Nusselt Number and flow stream function. From this analysis the heat transfer rate was compared each other and concludes that the higher heat transfer rate in square source than triangle source varying enclosures and different aspect ratio.

INTRODUCTION

The curiosity of natural convection in enclosures filled with air having cold vertical walls and adiabatic horizontal walls has been theme of research over the past years. The reason of considering this geometry is, it has application in various fields such as building and thermal insulation systems [1-7], solar engineering applications [8,9], geophysical fluid mechanics, etc...

The study of numerically the natural convection around tilted square cylinders in the range of ($0° \leq \theta \leq 45°$) inside an enclosure having horizontal adiabatic wall and cold vertical wall is studied. The investigated of the two dimensional natural convective flow and heat transfer around a heated cavity kept in a square enclosure in the range of $10^3 \leq Ra \leq 10^6$ [10-12]. Oosthuizen [13] has studied numerically the natural convective air flow in an enclosure with a horizontal lower wall, vertical side-walls and a straight inclined top wall. Sun [14] have investigated laminar natural convection heat transfer from a horizontal triangular cylinder to its concentric cylindrical enclosure. Fan [15] studied the effect of Prandtl number on the heat transfer in a horizontal cylindrical enclosure with a coaxial triangular cylinder inside it. Hussain and Hussein [16] investigated numerically the natural convection in a uniformly heated circular cylinder at different locations inside a square enclosure.

In the present work, the effect of size of a square and triangle bar in the square enclosure on the flow and heat transfer rate is compared for both the square and triangle sources according to the aspect ratio.

INVESTIGATION OF RESEARCH

The work is done systematically in a sequential manner to fulfill the research objective. Based on the objective of this study, literature survey was done. Available modeling techniques have been used for this purpose. The applied modeling techniques were of two types, mathematical and 2D modeling. The obtained results were keenly analyzed. Depending on the analysis output, results were elaborated and the final conclusion is provided **(Figure 1)**.

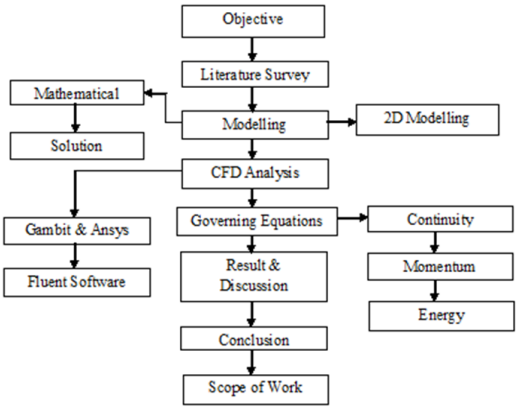

Figure 1. Work Plan Sequence.

MODELLING AND SIMULATION

Problem Definition

Figures 8 and 9 shows the geometry in which natural convective heat transfer is studied in the present work. Natural convection is the phenomenon where the movement of the fluid is characterised by the density changes. Here the natural convection is modelled with a heat source of square and triangle bar is placed inside an enclosure. Air is present between each of the heat source and the enclosure. Given the conditions of the different enclosure walls, the heat transfer is modelled. The aim is to study the best method that ensures the best heat transfer rate. The procedure is to be carried out with a different shape of the heat source and the heat transfer rate is studied. The problem is carried out in two-dimensional form.

Initially, the heat tranfer was studied for heated square bar domain and heated triangle bar domain by applying hot and cold sources **(Figures 2 and 3)**. Then the respective surface meshes of fluid around these bars were checked **(Figures 4 and 5)**.

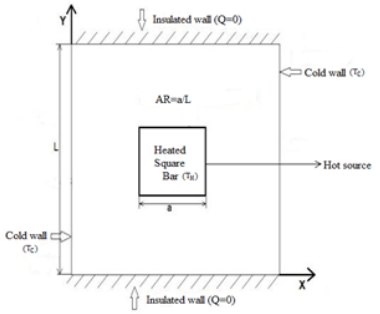

Figure 2. Computational Heated Square

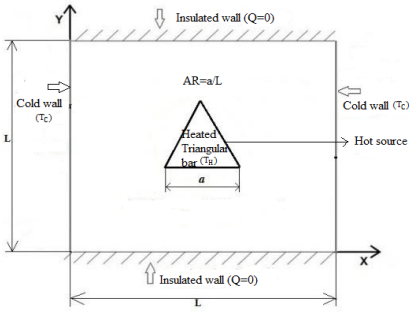

Figure 3. Computational Heated Triangle bar domain.

Boundary Condition for the Square Enclosure

The heat transfer was studied for the square enclosure by using different walls types, boundaries and conditions, which are represented in the following **Table 1**.

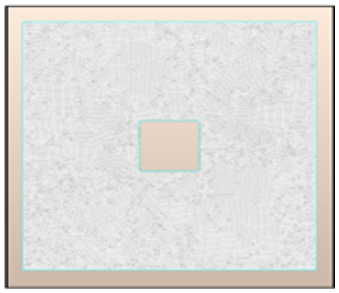

Figure 4. Surface mesh of fluid around Square bar.

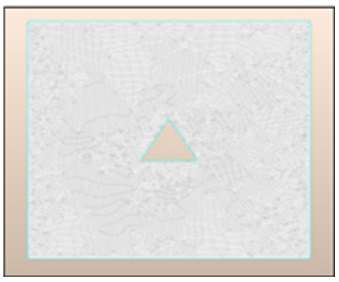

Figure 5. Surface mesh of fluid around Square bar.

Table 1. Boundary Condition for the Square Enclosure.

For the Square Enclosure		
Boundaries	**Wall Type**	**Condition**
Left side wall (T_c)	Cold	323.16 K
Right side wall (T_c)	Cold	323.16 K
Top wall	Adiabatic	Q = 0
Bottom wall	Adiabatic	Q = 0

SIMULATION FOR HEATED SQUARE BAR

A details simulation study was conducted for the square bar containing various lengths (L) and aspect ratios (A). These different length parameters and associated aspect ratios that were used for the square bar is shown individually as follows:

1. For the square bar enclosure of length L = 20 mm and Aspect ratio (A) = 0.2:

The simulation with length L= 20 mm and Aspect ratio (A) of 0.2 was studied and the results is provided in **Figures 6 and 7**, where **Figure 6** shows the contours of stream function and **Figure 7** shows velocity of fluid flow around square bar following the condition of A 0.2 and L 20 mm.

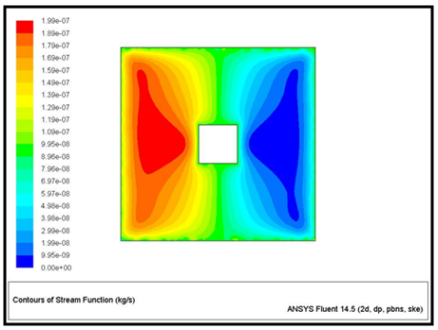

Figure 6. Contours of stream function aroun Square bar for A=0.2 and L= 20mm

2. For the square bar enclosure of length L = 20 mm and Aspect ratio (A) = 0:

The simulation study with length L= 20 mm and Aspect ratio (A) of 0.3 and the observed results is shown in **Figures 8 and 9**, where **Figure 8** depicts the contours of stream function and **Figure 9** represents velocity of fluid flow around square bar maintaining a value of A 0.2 and L 20 mm.

3. For the square bar enclosure of length L = 20 mm and Aspect ratio (A) = 0.4:

In continuation, similar simulation study was conducted with length L= 20 mm and Aspect ratio (A) = 0.4. The results are shown in **Figures 10 and 11**, where **Figure 10** shows the contours of stream function and **Figure 11** shows velocity of fluid flow around square bar of A 0.4 and L 20 mm.

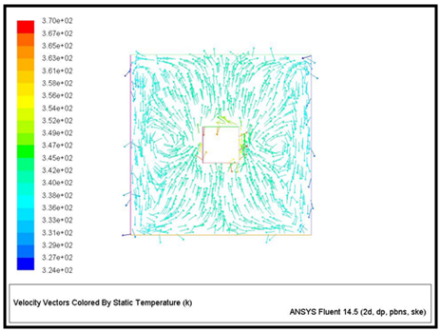

Figure 7. Velocity of fluid flow around square bar for A=0.2 and L=20mm.

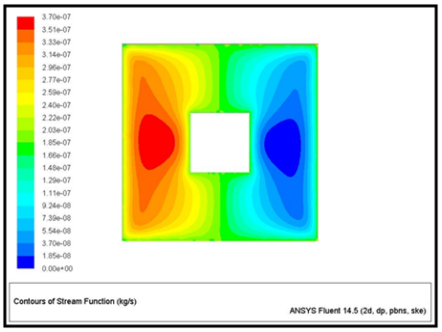

Figure 8. Contours of stream function aroundSquare bar for A=0.3 and L= 20mm.

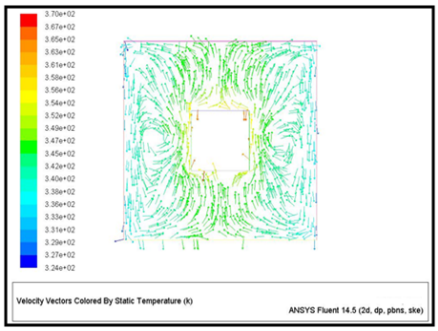

Figure 9. Velocity of fluid flow around square bar for A=0.3 and L=20mm.

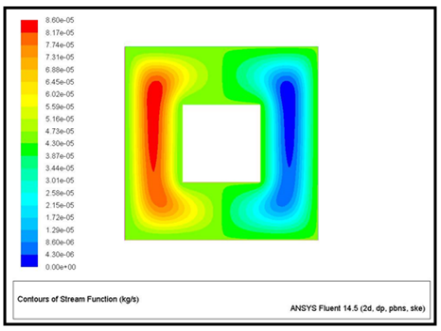

Figure 10. Contours of stream function around Square bar for A=0.4 and L= 20mm.

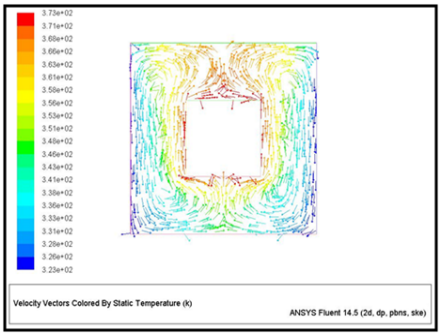

Figure 11. Velocity of fluid flow around square bar for A=0.4 and L=20mm.

4. For the square bar enclosure of length L = 40 mm and Aspect ratio (A) = 0.2:

Another parameter considered for the simulation was length L= 40 mm and Aspect ratio (A) = 0.2 and the results are shown in **Figures 12 and 13**, where **Figure 12** shows the contours of stream function and **Figure 13** shows velocity of fluid flow around square bar of A 0.2 and L 40 mm.

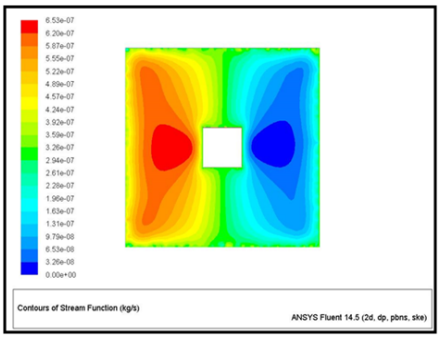

Figure 12. Contours of stream function around Square bar for A=0.2 and L= 40mm.

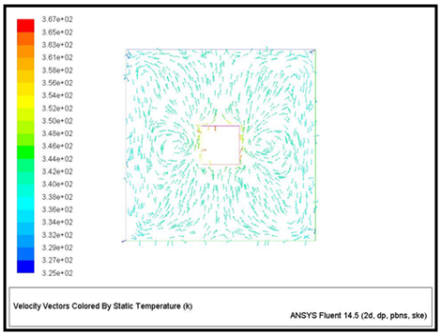

Figure 13. Velocity of fluid flow around square bar for A=0.2 and L=40mm.

5. For the square bar enclosure of length L = 40 mm and Aspect ratio (A) = 0.3:

The simulation with length L= 40 mm and Aspect ratio (A) = 0.3 was conducted whereas the secured results is shown in **Figures 14 and 15**, where **Figure 14** shows the contours of stream function and **Figure 15** shows velocity of fluid flow around square bar.

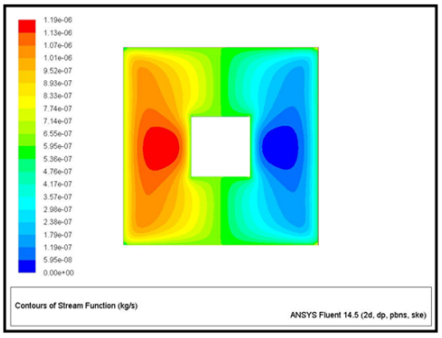

Figure 14. Contours of stream function around Square bar for A=0.3 and L= 40mm

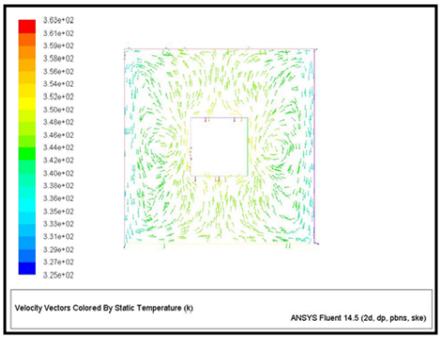

Figure 15. Velocity of fluid flow around square bar for A=0.3 and L=40mm.

6. For the square bar enclosure of length L = 40 mm and Aspect ratio (A) = 0:

The simulation with length L= 40 mm and Aspect ratio (A) = 0.4 was conducted whereas the secured results were shown

in **Figures 16 and 17**, where **Figure 16** shows the contours of stream function and **Figure 17** shows velocity of fluid flow around square bar of A 0.4 and L 40 mm.

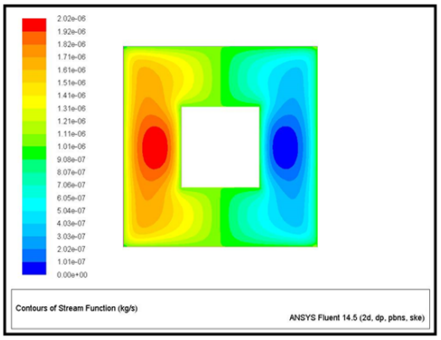

Figure 16. Contours of stream function around Square bar for A=0.4 and L= 40mm.

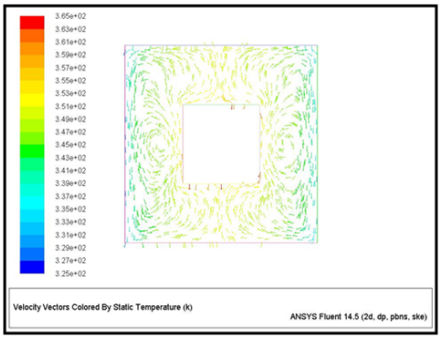

Figure 17. Velocity of fluid flow around square bar for A=0.4 and L=40mm.

7. For the square bar enclosure of length L = 80 mm and Aspect ratio (A) = 0.2:

The simulation with length L= 80 mm and Aspect ratio (A) = 0.2 were conducted whereas the secured results were shown in **Figures 18 and 19**, where **Figure 18** shows the contours of stream function and **Figure 19** shows velocity of fluid flow around square bar of A 0.2 and L 80 mm.

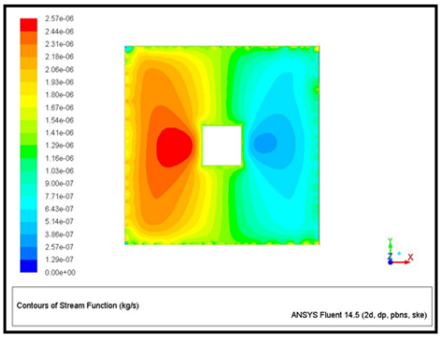

Figure 18. Contours of stream function around Square bar for A=0.2 and L= 80mm.

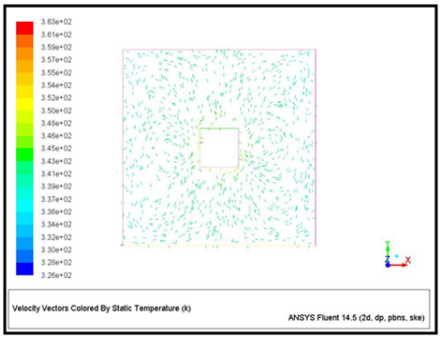

Figure 19. Velocity of fluid flow around square bar for A=0.2 and L=80mm.

8. For the square bar enclosure of length L = 80 mm and Aspect ratio (A) = 0.3:

The simulation with length L= 80 mm and Aspect ratio (A) = 0.3 were conducted and the secured results shown in **Figures 20 and 21**, where **Figure 20** shows the contours of stream function and **Figure 21** shows velocity of fluid flow around square bar of A 0.3 and L 80 mm.

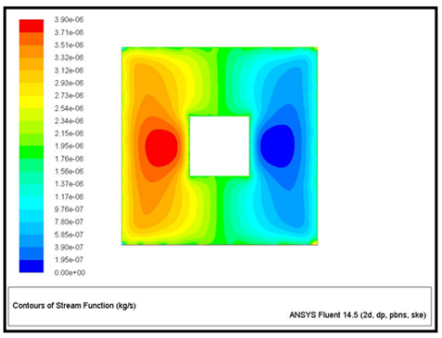

Figure 20. Contours of stream function around Square bar for A=0.3 and L= 80mm.

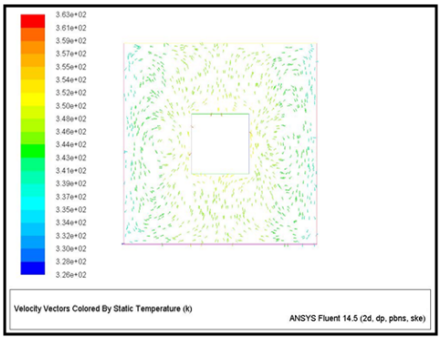

Figure 21. Velocity of fluid flow around square bar for A=0.3 and L=80mm.

9. For the square bar enclosure of length L = 80mm and Aspect ratio (A) = 0.4:

The simulation with length L= 80 mm and Aspect ratio (A) = 0.4 were conduct6ed and the secured results were shown in **Figures 22 and 23**, where **Figure 22** shows the contours of stream function and **Figure 23** shows velocity of fluid flow around square bar of A 0.4 and L 80 mm.

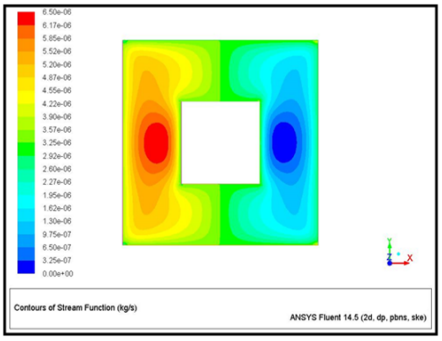

Figure 22. Contours of stream function around Square bar for A=0.4 and L= 80mm.

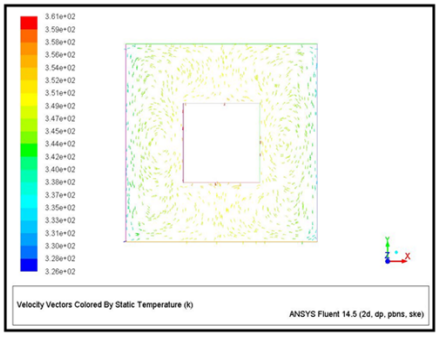

Figure 23. Velocity of fluid flow around square bar for A=0.4 and L=80mm.

SIMULATION FOR HEATED TRIANGLE BAR

The simulations for a heated triangle bar was studied with various lengths and aspect ratios. The results that were obtained, were shown individually as follows:

1. For the triangle bar enclosure of length L = 20 mm and Aspect ratio (A) = 0.2:

The simulation of heated triangle bar of length L = 20 mm and Aspect ratio (A) = 0.2 were conducted and the secured results

were shown in **Figures 23 and 24**. **Figure 23** shows the contours of stream function and **Figure 24** shows the velocity of fluid around the triangle bar.

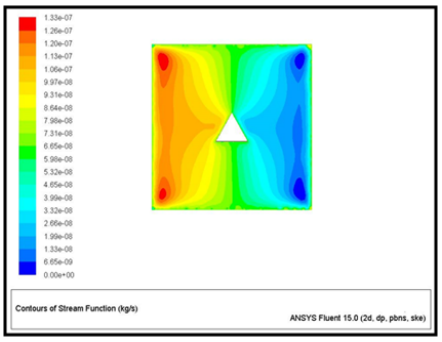

Figure 24. Contours of stream function around Triangle bar for A=0.2 and L= 20mm.

2. For the triangle bar enclosure of length L = 20 mm and Aspect ratio (A) = 0.3:

The simulation of heated triangle bar of length L = 20 mm and Aspect ratio (A) = 0.3 were conducted and the secured results were shown in **Figures 25-27**. **Figure 26** shows the contours of stream function and **Figure 27** shows the velocity of fluid around the triangle bar.

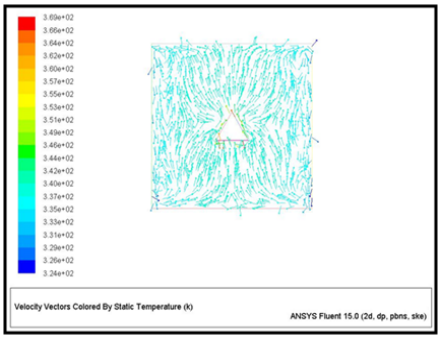

Figure 25. Velocity of fluid flow around Triangle bar for A=0.2 and L=20mm.

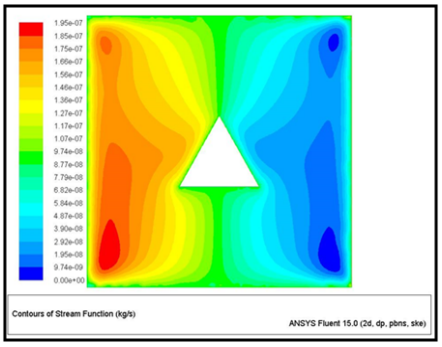

Figure 26. Contours of stream function around Triangle bar for A=0.3 and L= 20mm.

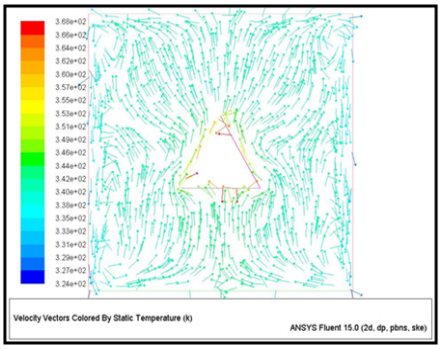

Figure 27. Velocity of fluid flow around Triangle bar for A=0.3 and L=20mm.

3. For the triangle bar enclosure of length L = 20 mm and Aspect ratio (A) = 0.4:

The simulation of heated triangle bar of length L = 20 mm and Aspect ratio (A) = 0.4 were studied and the secured results were shown in **Figures 28 and 29**. **Figure 28** shows the contours of stream function and **Figure 29** shows the velocity of fluid around the triangle bar.

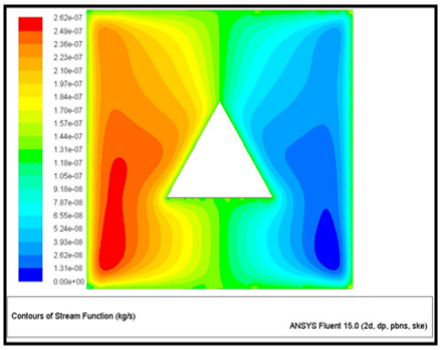

Figure 28. Contours of stream function around Triangle bar for A=0.4 and L= 20mm.

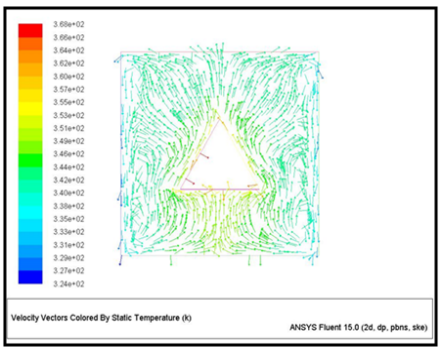

Figure 29. Velocity of fluid flow around Triangle bar for A=0.4 and L=20mm.

4. For the triangle bar enclosure of length L = 40 mm and Aspect ratio (A) = 0.2:

The simulation of heated triangle bar of length L = 40 mm and Aspect ratio (A) = 0.2 were conducted and the secured results were shown in **Figures 30 and 31**. **Figure 30** shows the contours of stream function and **Figure 31** shows the velocity of fluid around the triangle bar.

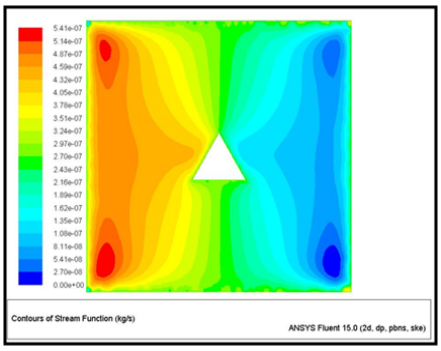

Figure 30. Contours of stream function around Triangle bar for A=0.2 and L= 40mm.

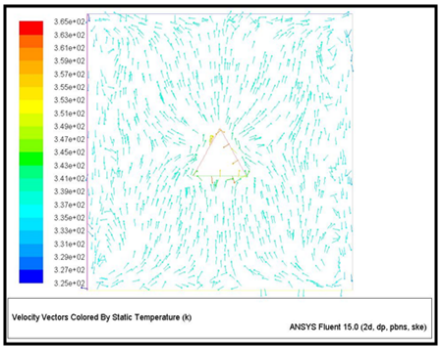

Figure 31. Velocity of fluid flow around Triangle bar for A=0.2 and L=40mm.

5. For the triangle bar enclosure of length L = 40 mm and Aspect ratio (A) = 0.3:

The simulation of heated triangle bar of length L = 20 mm and Aspect ratio (A) = 0.2 were conducted and the secured results were shown in **Figures 32 and 33**. **Figure 32** shows the contours of stream function and **Figure 33** shows the velocity of fluid around the triangle bar.

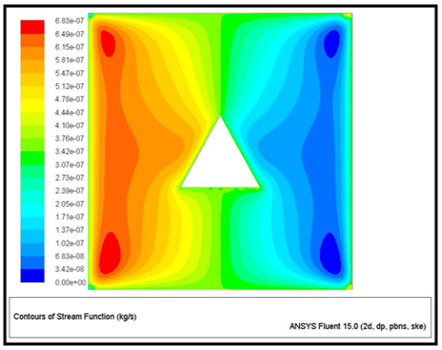

Figure 32. Contours of stream function around Triangle bar for A=0.3 and L= 40mm.

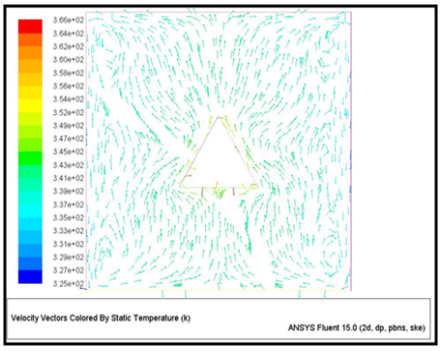

Figure 33. Velocity of fluid flow around Triangle bar for A=0.3 and L=40mm

6. For the triangle bar enclosure of length L = 40 mm and Aspect ratio (A) = 0.4:

The simulation of heated triangle bar of length L = 40 mm and Aspect ratio (A) = 0.4 were conducted and the secured results were shown in **Figures 34 and 35**. **Figure 34** shows the contours of stream function and **Figure 35** shows the velocity of fluid around the triangle bar.

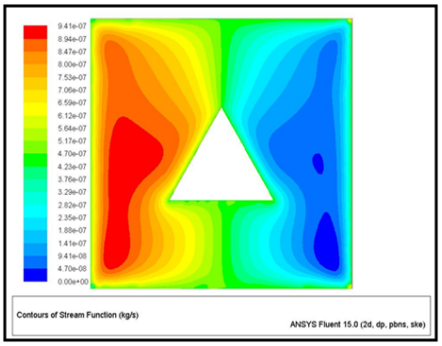

Figure 34. Contours of stream function around Triangle bar for A=0.4 and L= 40mm.

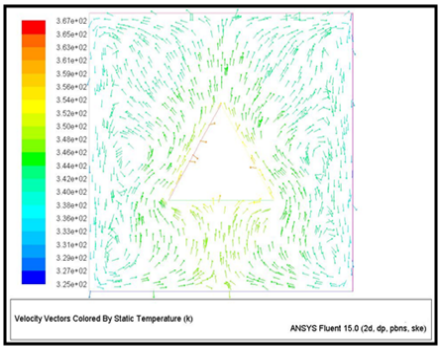

Figure 35. Velocity of fluid flow around Triangle bar for A=0.4 and L=40mm.

7. For the triangle bar enclosure of length L = 80 mm and Aspect ratio (A) = 0.2:

The simulation of heated triangle bar of length L = 80 mm and Aspect ratio (A) = 0.2 were conducted and the secured results were shown in **Figures 36 and 37. Figure 36** shows the contours of stream function and **Figure 37** shows the velocity of fluid around the triangle bar.

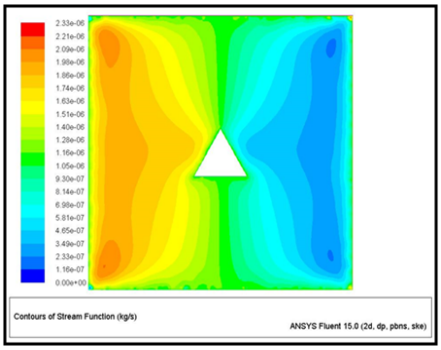

Figure 36. Contours of stream function around Triangle bar for A=0.2 and L= 80mm.

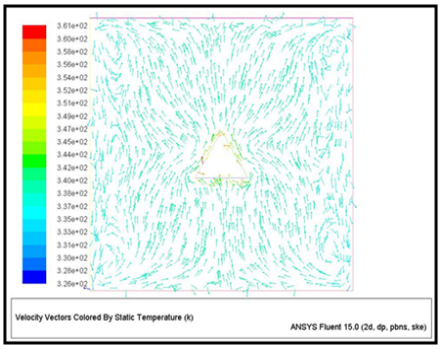

Figure 37. Velocity of fluid flow around Triangle bar for A=0.2 and L=80mm.

8. For the triangle bar enclosure of length L = 80 mm and Aspect ratio (A) = 0.3:

The simulation of heated triangle bar of length L = 80 mm and Aspect ratio (A) = 0.3 were conducted and the secured results were shown in **Figures 38 and 39**. **Figure 38** shows the contours of stream function and **Figure 39** shows the velocity of fluid around the triangle bar.

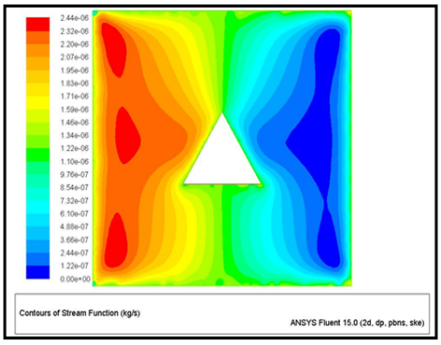

Figure 38. Contours of stream function around Triangle bar for A=0.3 and L= 80mm.

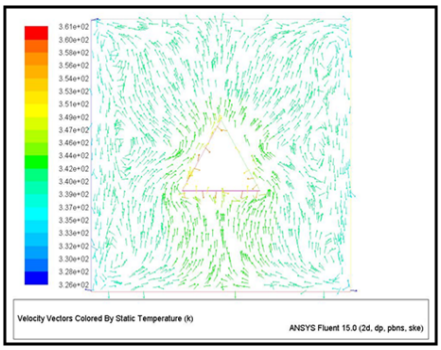

Figure 39. Velocity of fluid flow around Triangle bar for A=0.3 and L=80mm.

9. For the triangle bar enclosure of length L = 80 mm and Aspect ratio (A) = 0.4:

The simulation of heated triangle bar of length L = 80 mm and Aspect ratio (A) = 0.4 were conducted and the secured results were shown in **Figures 40 and 41**. **Figure 40** shows the contours of stream function and **Figure 41** shows the velocity of fluid around the triangle bar.

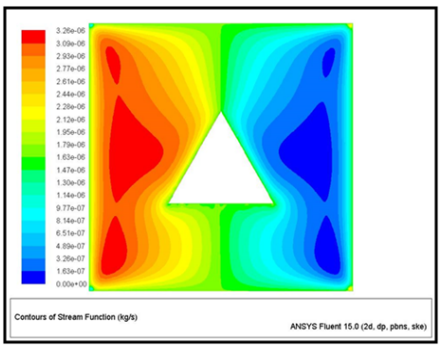

Figure 40. Contours of stream function around Triangle bar for A=0.4 and L= 80mm.

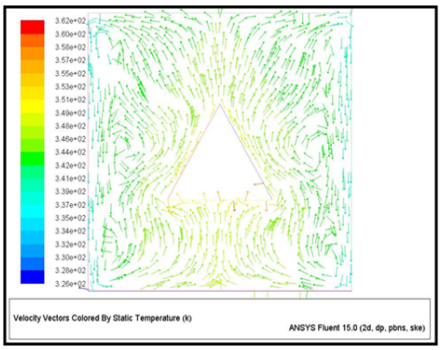

Figure 41. Velocity of fluid flow around Triangle bar for A=0.4 and L=80m

RESULT AND DISCUSSION

From the above work, the results that were obtained is shown in **Tables 2 and 3**. The obtained results for a square bar of varying lengths and aspect ratios are represeted in an understandable manner. From the above results obtained, variations in Nusselt no. and enclosure left wall were estimated.

Table 2. Boundary Condition for the hot sources.

For the hot sources		
Boundaries	**Wall Type**	**Condition**
All the four sides of square bar (T_H)	Heated wall	373.16 K
All the three sides of triangle bar (T_H)	Heated wall	373.16 K

Table 3. Result obtained for square bar by varying enclosure lengths and aspect ratio.

Enclosure Length in mm	Aspect Ratio	Heat Transfer Q in watts	Heat Transfer Coefficient h in W/m²K	Nusselt number Nu
20	0.2	13.38	19.677	1.626
	0.3	18.079	35.449	2.197
	0.4	19.059	56.057	2.316
40	0.2	24.305	17.872	2.594
	0.3	29.217	28.644	3.551
	0.4	30.442	44.768	3.7
80	0.2	38.236	14.056	4.647
	0.3	43.694	32.128	5.31
	0.4	43.942	21.539	5.34

Nusselt Number

The Nusselt number (Nu) is the ratio of convective to conductive heat transfer across the boundary. In this context, convection includes both advection and diffusion. It is calculated for a heat transfer across a boundary within a fluid. The conductive component is measured under the same conditions as the heat convection but with a (hypothetically) stagnant (or motionless) fluid.

The variations of Nusselt number and enclosure side wall of square and triangle bars of various lengths were estimated as shown in following **Figures 42-56**. The results obtained for a triangle bar with varying lengths and aspect ratios can be shown in **Table 4**. For determining the variation of Nusselt number with enclosure of wall was determined for both square and triangular bars by using various lengths of 20, 40 and 80 mm.

Square Bar

1. For the square bar enclosure of length L=20 mm (Figures 43-45):

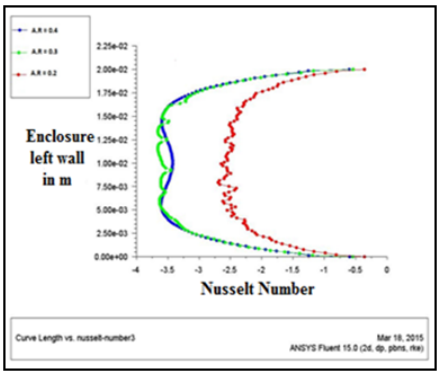

Figure 42. Variation of Nusselt number and Enclosure left wall.

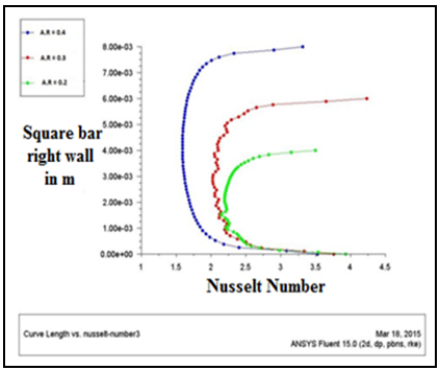

Figure 43. Variation of Nusselt number and Square bar right wall.

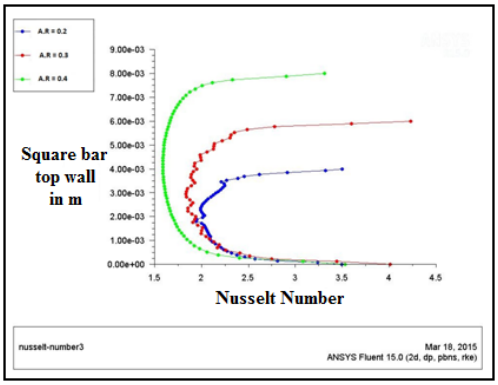

Figure 44. Variation of Nusselt number and Square bar top wall.

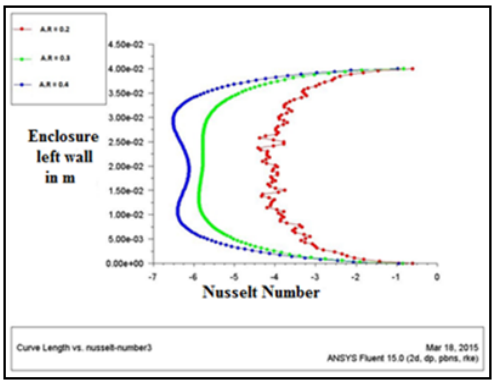

Figure 45. Variation of Nusselt number and Enclosure left wall.

2. For the square bar enclosure of length L=40 mm (Figures 46-49):

3. For the square bar enclosure of length L=80 mm (Figures 48-50) (Table 4):

Triangle Bar

1. For the triangle bar enclosure of length L=20mm (Figures 51 and 52):

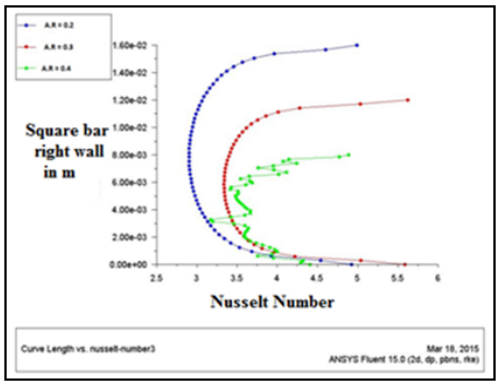

Figure 46. Variation of Nusselt number and Square bar right wall.

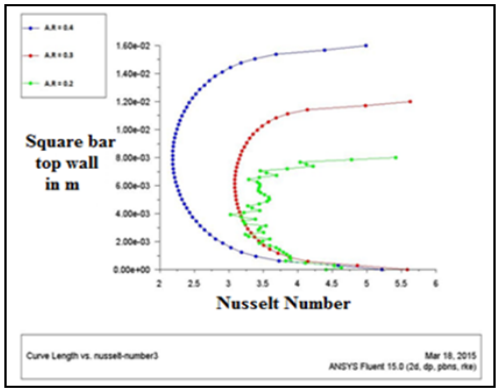

Figure 47. Variation of Nusselt number and Square bar top wall.

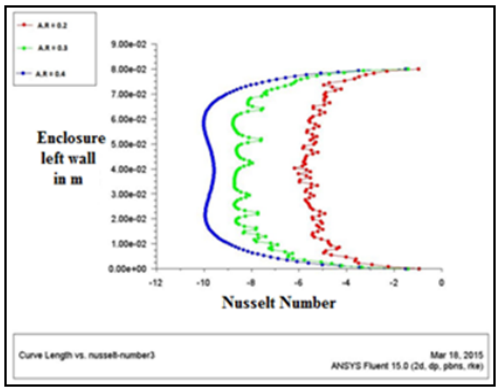

Figure 48. Variation of Nusselt number and Enclosure left wall.

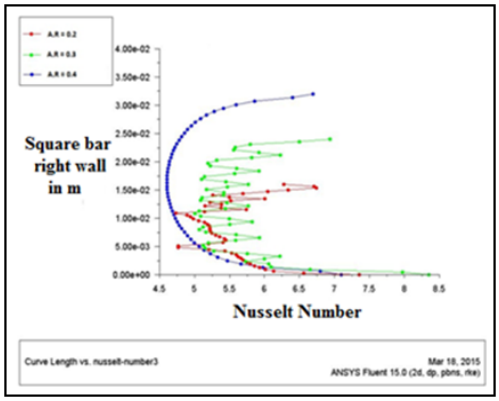

Figure 49. Variation of Nusselt number and Square bar right wall.

2. For the triangle bar enclosure of length L=40mm (Figure 53 and 54):

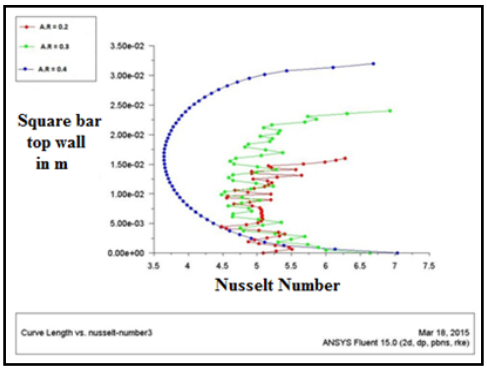

Figure 50. Variation of Nusselt number and Square bar top wall.

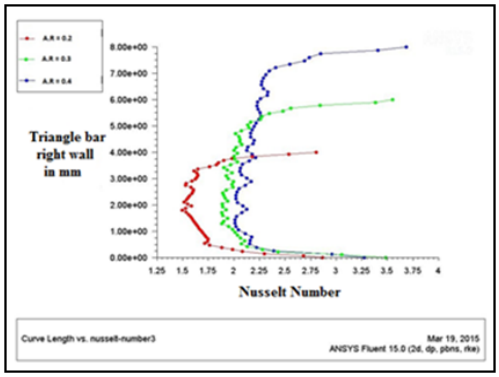

Figure 51. Variation of Nusselt number and Triangle bar right wall.

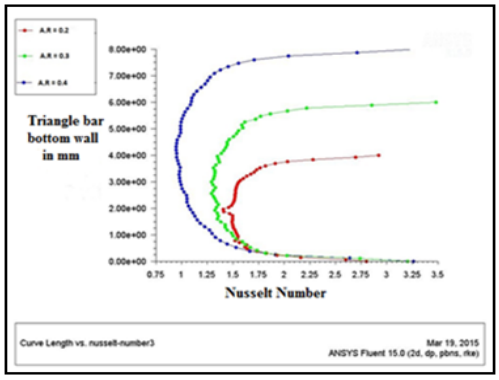

Figure 52. Variation of Nusselt number andTriangle bar bottom wall.

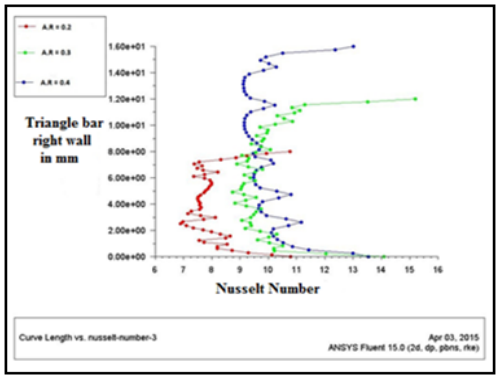

Figure 53. Variation of Nusselt number and Triangle bar right wall.

3. For the triangle bar enclosure of length L=80mm (Figure 55 and 56):

CONCLUSION

Heat transfer and fluid flow due to natural convection in air around heated square cylinders of different sizes inside an enclosure having adiabatic horizontal and diathermic vertical walls of size 20 mm, 40 mm and 80 mm with respect to aspect ratio of 0.2, 0.3 and 0.4 are analyzed, and results are exhibited in the dimension form of Stream function and Velocity vector diagram.

The fluid motion and circulation rate increase with increase in enclosure size. The fluid motion is almost uniform for lower

for smaller enclosure size and the fluid motion is prominent near the walls and the fluid is almost stagnant in the core region for higher larger enclosure size. The heat transfer rate is comparatively higher at the upper portions of the vertical enclosure walls and from the base of the triangle bar. For smaller enclosures, the circulation rate decreases with increase in bar size, but for larger enclosure, the circulation rate increases with bar size.

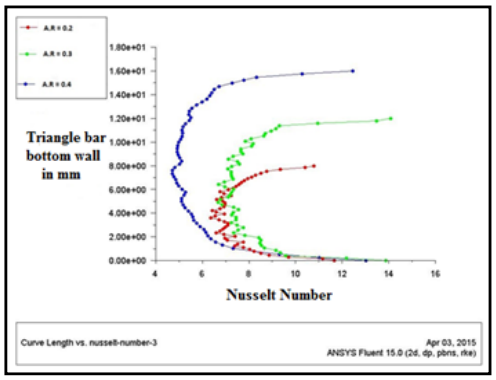

Figure 54. Variation of Nusselt number and Triangle bar bottom wall.

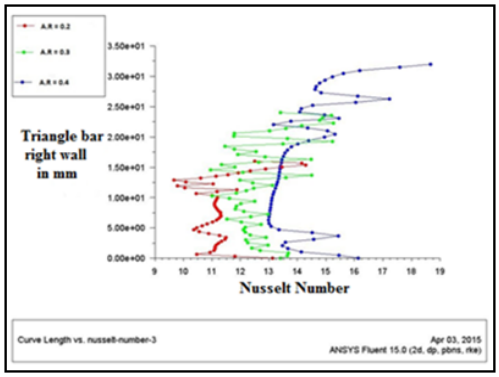

Figure 55. Variation of Nusselt number and Triangle bar right wall.

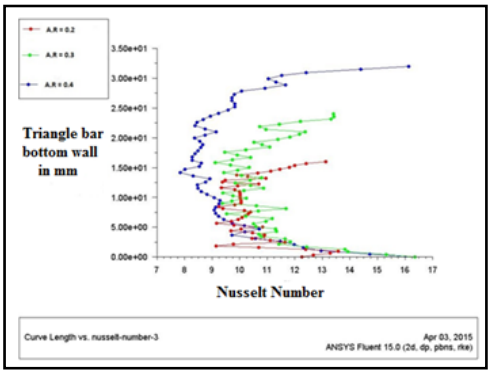

Figure 56. Variation of Nusselt number andTriangle bar bottom wall.

Table 4. Result obtained for triangle bar by varying enclosure lengths and aspect ratio.

Enclosure Length in mm	Aspect Ratio	Heat Transfer Q in watts	Heat Transfer Coefficient h in W/m²K	Nusselt number Nu
20	0.2	24.652	72.507	1.723
	0.3	26.108	38.394	1.85
	0.4	26.456	51.877	1.905
40	0.2	37.458	54.776	2.64
	0.3	40.55	29.816	2.823
	0.4	41.933	41.111	3.114
80	0.2	52.687	38.74	40106
	0.3	58.379	28.617	4.244
	0.4	60.954	22.41	3.668

It's proved that Nusselt number dependent of temperature and heated source bar can absorb more energy by increasing the size and can transfer more heat to the diathermic walls for various purposes.

REFERENCES

1. Akinsete VA and Coleman TA. Heat transfer by steady laminar free convection in triangular enclosures, Int. J. Heat Mass Transfer 1982; 25: 991–998.
2. Holtzman GA, et al. Laminar natural convection in isosceles triangular enclosures heated from below and symmetrically cooled from above, J. Heat Transfer – Trans. ASME, 2000; 485–491.
3. Haese PM and Teubner MD. Heat exchange in an attic space, Int. J. Heat Mass Transfer 2002; 45:4925–4936.
4. Saha SC. Unsteady natural convection in a triangular enclosure under isothermal heating, Energy Build 2011; 43:695–703.
5. Saha SC. Scaling of free convection heat transfer in a triangular cavity for Pr > 1, Energy Build 2011;43: 2908–2917.
6. Saha SC, et al. Natural convection in attics subject to instantaneous and ramp cooling boundary conditions, Energy Build 2010; 42:1192–1204.
7. Saha SC, et al. Natural convection in attic-shaped spaces subject to sudden and ramp heating boundary conditions, Heat Mass Transfer 2010;46:621–638.
8. Joudi KA, et al. Computational model for a prism shaped storage solar collector with a right triangular cross section, Energy Convers. Manage 2004; 45:337–342.
9. Kaushik SC, et al. Transient analysis of a triangular built-in-storage solar water-heater under winter conditions, Heat Recovery Syst. 1994; 14:391–409.
10. Roychowdhury DG, et al. Numerical simulation of natural convective heat transfer and fluid flow around a heated cylinder inside an enclosure, Heat Mass Transfer 2002;38: 565–576.
11. Dalal A, et al. Natural convection around a heated square cylinder placed in different angles inside an enclosure, Heat and mass transfer conference 2008; 45.
12. De K and Dalal A. A numerical study of natural convection around a square horizontal heated cylinder placed in an enclosure, International Journal of Heat and Mass Transfer 2006;49:4608-4623.
13. Oosthuizen PH. Free convective flow in an enclosure with a cooled inclined upper surface, Computational mechanics 1994; 14:420-430.
14. Xu X, et al. Numerical investigation of laminar natural convective heat transfer from a horizontal triangular cylinder to its concentric cylindrical enclosure, International Journal of Heat and Mass Transfer 2009;52:3176–3186.
15. Yu Z, et al. Prandtl number dependence of laminar natural convection heat transfer in a horizontal cylindrical enclosure with an inner coaxial triangular cylinder, International Journal of Heat and Mass Transfer 2010; 53: 1333–1340.
16. Hussain S and Hussein K. Numerical investigation of natural convection phenomena in a uniformly heated circular cylinder immersed in square enclosure filled with air at different vertical locations, International Communications in Heat and Mass Transfer 2010;37:1115–1126.